International Journal of Pharmaceutics 426 (2012) 193–201

Contents lists available at SciVerse ScienceDirect

International Journal of Pharmaceutics

journal homepage: www.elsevier.com/locate/ijpharm

Pharmaceutical Nanotechnology

Reversion of multidrug resistance by co-encapsulation of doxorubicin and curcumin in chitosan/poly(butyl cyanoacrylate) nanoparticles

Jinghua Duan[a,b], Heidi M. Mansour[b], Yangde Zhang[a], Xingming Deng[c], Yuxiang Chen[a], Jiwei Wang[a], Yifeng Pan[a], Jinfeng Zhao[a,*]

[a] The National Hepatobiliary & Enteric Surgery Research Center, Xiangya Hospital, Central South University, Changsha, Hunan 410008, PR China
[b] Department of Pharmaceutical Sciences – Drug Development Division, College of Pharmacy, University of Kentucky, Lexington, KY 40536-0596, USA
[c] Division of Cancer Biology and Department of Radiation Oncology, Emory University School of Medicine, Atlanta, GA 30322, USA

ARTICLE INFO

Article history:
Received 4 November 2011
Received in revised form
27 December 2011
Accepted 9 January 2012
Available online 17 January 2012

Keywords:
Curcumin
Doxorubicin
Poly(butyl cyanoacrylate) nanoparticles
Multidrug resistance

ABSTRACT

Co-encapsulated doxorubicin (DOX) and curcumin (CUR) in poly(butyl cyanoacrylate) nanoparticles (PBCA-NPs) were prepared with emulsion polymerization and interfacial polymerization. The mean particle size and mean zeta potential of CUR–DOX–PBCA-NPs were 133 ± 5.34 nm in diameter and +32.23 ± 4.56 mV, respectively. The entrapment efficiencies of doxorubicin and curcumin were 49.98 ± 3.32% and 94.52 ± 3.14%, respectively. Anticancer activities and reversal efficacy of the formulations and various combination approaches were assessed using 3-[4,5-dimethylthiazol-2-yl] 2,5-diphenyltetrazolium bromide assay and western blotting. The results showed that the dual-agent loaded PBCA-NPs system had the similar cytotoxicity to co-administration of two single-agent loaded PBCA-NPs (DOX–PBCA-NPs + CUR–PBCA-NPs), which was slightly higher than that of the free drug combination (DOX + CUR) and one free drug/another agent loaded PBCA-NPs combination (DOX + CUR–PBCA-NPs or CUR + DOX–PBCA-NPs). The simultaneous administration of doxorubicin and curcumin achieved the highest reversal efficacy and down-regulation of P-glycoprotein in MCF-7/ADR cell lines, an MCF-7 breast carcer cell line resistant to adriamycin. Multidrug resistance can be enhanced by combination delivery of encapsulated cytotoxic drugs and reversal agents.

1. Introduction

Multidrug resistance (MDR), whereby cancer cells become resistant to the cytotoxic effects of various structurally and mechanistically unrelated chemotherapeutic agents, is a major problem in the clinical treatment of cancer. Doxorubicin (DOX) is an effective chemotherapeutic agent, which has been used extensively for treatment of various cancers, particular for breast cancer, lymphoma and hematological cancers. Unfortunately, many tumor cells are not sensitive to DOX because of efflux from the tumor cells mediated by P-glycoprotein (P-gp), multidrug resistance-associated protein 1 (MRP1), topoisomerase II (Topo II) and glutathione transferase (GST-π) (Lage, 2003). Meanwhile, DOX also has severe cardiovascular toxicity when administered systemically (Gu et al., 2007), which can limit therapeutic efficacy in cancer patients. Nanomedicines and nanoparticles for nanopharmaceutical delivery have demonstrated advantages in enhancing chemotherapeutic delivery in drug-resistant cancers (Chen et al., 2008; Song et al., 2009; Kang et al., 2010; Dong et al., 2009; Wu et al., 2007; Tang et al., 2010; Dong and Mumper, 2010).

Curcumin (CUR), a naturally occurring polyphenol extracted from the rhizome Curcuma longa, has a long history of use as an Asian spice as well as in traditional therapies. Exciting recent studies have shown that curcumin, either alone or in combination with other anticancer agents, has a pleiotropic therapeutic effect in cancer (Notarbartolo et al., 2005). Additionally, CUR is also known to downregulate the intracellular levels of three major ATP-binding cassette (ABC) drug transporters, P-gp, MRP-1 and mitoxantrone resistance protein (ABCG2), that are important in MDR (Antonio et al., 2008; Hou et al., 2008; Ebert et al., 2007; Andjelkovic et al., 2008). This pleiotropic effect of CUR is especially advantageous when administered with a delivery system that enhances bioavailability at the tumor mass and promote intracellular availability of the combination drugs upon systemic administration. Previous research (Notarbartolo et al., 2005) also demonstrated that curcumin in combination with doxorubicin could result in better treatment efficacy. Amiij found that the co-administering of an antitumor agent and a reversion agent affected the efficacy of resistance reversion and also demonstrated that simultaneous administration of curcumin and paclitaxel could result in better treatment efficacy (Ganta and Amiji, 2009). Curcumin has been

* Corresponding author. Tel.: +86 731 84327971; fax: +86 731 84327987.
E-mail addresses: zhaojinfeng@hotmail.com, bax_2007@126.com (J. Zhao).

0378-5173/$ – see front matter © 2012 Elsevier B.V. All rights reserved.
doi:10.1016/j.ijpharm.2012.01.020

found to be safe, with no dose-limiting toxicity, when administered at doses up to 10 g/day in humans (Cheng et al., 2001). However, curcumin undergoes rapid and extensive metabolism in the liver and intestine and demonstrates poor bioavailability; thereby limiting its usefulness as a potent chemopreventive agent (Anand et al., 2007).

Biodegradable and biocompatible polymers are often used for controlled release of drugs, in advanced drug delivery systems, and approved pharmaceutical products that are commercially available. In the past two decades, poly(butyl cyanoacrylate) (PBCA) has been extensively used in drug delivery systems for a variety of drugs due to its excellent biocompatibility and biodegradability. Current literature is replete with studies investigating single-agent incorporation into PBCA nanoparticles (Ambruosi et al., 2006; Reddy et al., 2004; Sullivan and Birkinshaw, 2004; Behan et al., 2001; Wohlgemuth et al., 2000), while PBCA nanoparticles loaded with dual agents were reported scarcely. In this study, doxorubicin hydrochloride (DOX·HCl) and curcumin are hydrophilic and hydrophobic molecules, respectively. Owing to the very different properties of the two drugs, preparing the dual drug-loaded PBCA nanoparticles with high drug entrapment efficiency using the adapted preparation method presents a real challenge. The commonly reported preparation methods of PACA nanoparticles include emulsion polymerization, interfacial polymerization, nanoprecipitation and emulsification-solvent evaporation (Vauthier et al., 2003). Taking into account the properties of CUR and DOX, the emulsion polymerization and interfacial polymerization were selected for this study.

In this study, it may be preferable to prepare nanoparticles incorporated with both CUR and DOX so that the two substances could be delivered simultaneously. The formulation parameters were systematically investigated. Thus, nanoparticles with some expectable properties such as high drug entrapment efficiency and small size can be produced through the optimized formulation. Subsequently, the physicochemical characteristics were also evaluated, which can provide some useful and essential information for *in vitro* cell experiments and *in vivo* studies. Thus, the co-encapsulation of DOX and CUR should diminish side effects of both drugs while increasing efficacy. Furthermore, it should reduce the amount of the polymer needed for a single formulation as compared to the amount of polymer required in two separate nanoparticle dosage forms, allowing for a better safety profile of the combined formulation. Recently published studies demonstrated that poly(alkyl cyanoacrylate) nanoparticles can overcome MDR at both the cellular and the non-cellular level (De Verdiere et al., 1997). Thus, co-encapsulating CUR and DOX in PBCA nanoparticles might overcome MDR through the chemosensitizer CUR and the carrier PBCA nanoparticles. In addition, their cytotoxicity was verified on MCF-7 doxorubicin resistant cell line.

2. Materials and methods

2.1. Materials

Chitosan (degree of deacetylation ≥85%) was purchased from Sigma corporation. Butyl cyanoacrylate (BCA) monomer was synthesized by Guangzhou Baiyun Medical Adhensive Co., Ltd. (Guangzhou, China). Curcumin was obtained from Sinopharm Chemical Reagent Co., Ltd. (Shanghai, China). Doxorubicin Hydrochloride was purchased from National Institute for the control of Pharmaceutical and Biological Products (Beijing, China). Gradient-grade methanol were purchased from Merck (Germany) and used as received. 3-[4,5-Dimethylthiazol-2-yl] 2,5-diphenyltetrazolium bromide (MTT reagent) was purchased from Trevigen, Inc. (USA). Anti-MDR1 rabbit polyclonal antibody, anti-MRP1 rabbit polyclonal antibody and anti-ABCG2 rabbit polyclonal antibody, which were obtained from Boster Biological Technology, Ltd. (Wuhan, China). All other chemicals used were of analytical reagent grade and without further purification. Ultrapure water was used for the preparation of all solutions.

2.2. Tumor cell lines and culture

A human breast carcinoma cell line, MCF-7, and its adriamycin-resistant variant, MCF-7/ADR, induced by doxorubicin and expresses a high level of P-gp, were purchased from Nanjing KeyGen Biotech. Co. Ltd. (China). RPMI-1640 medium, newborn calf serum (NBCS), penicillin/streptomycin and 0.25% trypsin were obtained from Gibco, Invitrogen Corporation (Canada). Cells were grown in RPMI 1640 medium, supplemented with 10% newborn calf serum and 1% penicillin/streptomycin.

2.3. Preparation and optimization of drug loaded chitosan–PBCA nanoparticles

PBCA nanoparticles loaded with CUR and DOX were prepared using emulsion polymerization and interfacial polymerization as previously reported, obtained by anionic polymerization at pH below 3 (Vauthier et al., 2003; Duan et al., 2010). Since BCA is an extremely active monomer, even the presence of a weak basic substance is capable of initiating the anionic polymerization. Here, we used chitosan as a stabilizing agent. Chitosan-containing amino and hydroxyl groups might act as nucleophilic agents to initiate the butyl cyanoacrylate monomer. In this case, DOX was first added in the aqueous polymerization medium, then at different time intervals (15, 30, 60 and 120 min) after the polymerization process was initiated, 1 mL of alcohol solution of curcumin (1 mg/mL) was injected after the monomer BCA was introduced. Butyl cyanoacrylate monomer was added to a solution of chitosan in the polymerization medium containing HCl. The overall polymerization process lasted over 6 h. After 6 h the nanoparticle suspension is neutralized with 0.5 mol/L NaOH. The nanoparticles were separated by ultracentrifugation at 16,000 rpm (Sigma 3K-18 refrigerated centrifuge, Germany) for 30 min and washed with distilled water at least three times.

Because the temperature and stirring speed have little effect on the formation of poly(butyl cyanoacrylate) (Vauthier et al., 2003). In this study, the effect of various processing parameters and polymer characteristics on nanoparticles mean diameter, zeta potential, drug loading and entrapment efficiencies were assessed, including the chitosan concentration in the aqueous phase, the amount of butyl cyanoacrylate monomer in polymerization phase, initial CUR and DOX content. Unless otherwise mentioned, all the experiments were conducted by varying one of the parameters while keeping all the other process parameters at a set of standard conditions: Briefly, 1% (w/v) BCA was added under mechanical stirring to an aqueous polymerization medium (0.01% (w/v) chitosan, 50 μL HCl). 1 mL of 1 mg/mL DOX was added in the polymerization medium at the beginning of the process. Then, 1 mL alcohol solution of CUR (1 mg/mL) was introduced 1 h after the polymerization process was initiated.

2.4. Particle size and zeta potential

CUR–DOX–PBCA nanoparticle suspensions were diluted with deionized water to ensure that the signal intensity was suitable for the instrument. Values are presented as mean ± SD from three replicate samples.

Particle size was determined by photon correlation spectroscopy (PCS) using Zetasizer Nano ZS (Malvern Instruments Ltd., Malvern, UK). The colloidal suspension of the nanoparticles was diluted with deionized distilled water, and the intensity

of scattered light was detected at a scattering angle of 173° to an incident beam at a temperature of 25 °C. The polydispersity index range was comprised between 0 and 1. Zeta potential was measured using the same instrument at 25 °C following the same dilution in a 10 mmol/L NaCl solution. The mean zeta potential was determined using phase analysis light scattering technique.

2.5. Transmission electron microscopy

The surface appearance and shape of CUR–DOX–PBCA nanoparticles were observed by transmission electron microscopy (TEM) using a JEOL-1230 (Japan) at 100 kV. 1 mL dispersion was diluted with 1 mL deionized water and a drop of it was placed onto a collodion support on copper grids (200 mesh). About 2 min of deposition, the grid was tapped with a filter paper to remove surface water and negatively stained by using a sodium phosphotungstate for 2 min. After 1 min, excess fluid was removed and the grid surface was air-dried at room temperature before being loaded in the microscope.

2.6. Drug loading and encapsulation efficiencies

An HPLC system (P680 series, DIONEX, USA) was used to separate doxorubicin and curcumin incorporated in the nanoparticles, with column Hypersil BDS C18 (4.6 mm × 250 mm, 5 μm) and the mobile phase consisted of methanol and 5% (w/v) of acetic acid at the volume ratio of 80:20. The flow rate was set at 1.0 mL/min and the analysis wavelength was at 420 nm. All the analysis was performed at 30 °C. Nonencapsulated doxorubicin and curcumin were separated by ultracentrifugation of the suspension at 16,000 rpm for 30 min. The supernatant was decanted and 20 μL of sample was injected into a DIONEX P680 liquid chromatograph to determine the actual amounts of CUR and DOX incorporated within the nanoparticles.

The drug encapsulation capacity of doxorubicin and curcumin was defined as the ratio of the mass of the encapsulated drug to the mass of the drug used for nanoparticles preparation using the following equation:

$$\text{Encapsulation capacity (EC\%)} = \frac{\text{the amount of loaded doxorubicin or curcumin}}{\text{total amount of doxorubicin or curcumin used for nanoparticles preparation}} \times 100.$$

The loading doxorubicin and curcumin content in the nanoparticles was calculated using the following equation:

$$\text{Drug loading (DL\%)} = \frac{\text{the amount of loaded doxorubicin or curcumin}}{\text{totoal amount of the preparation DOX–CUR-PBCA NPs}} \times 100.$$

2.7. Fourier transform infrared spectrometer

The nanoparticle functionalization was examined by Fourier transform infrared (FTIR) spectroscopy. The FTIR spectra of free doxorubicin, free curcumin, blank PBCA nanoparticles, CUR–DOX–PBCA nanoparticles and the physical mixture of doxorubicin, curcumin and blank PBCA nanoparticles were recorded on a TENSOR 27 FTIR spectrometer (Bruker, Billerica, MA, USA) at 4 cm^{-1} resolution in the transmission mode. Nanoparticle powders (2 mg) were gently mixed with KBr and the mixture was pressed into a pellet for analysis. The FTIR spectrum was measured in the 400–4000 cm^{-1} region for sample dispersed in KBr pellets.

2.8. Determination of the molecular weight of the nanoparticles

Molecular weights for the various kinds of PBCA nanoparticles was determined by gel permeation chromatography (Waters 1515, USA) with refractive index detector (Waters 2414) and using THF as the mobile phase. The flow rate and temperature was maintained at 1 mL/min and 30 °C respectively. Freeze-dried drug-loaded nanoparticles were dissolved in THF at a polymer concentration of 1% and filtered through a membrane filter of 0.45 μm pore size. 20 μL of this solution was injected into the chromatograph. Polystyrene standards of 462,000, 186,000, 114,000, 43,700, 18,600, 9650, 6520, 2950 and 461 Da were used for column calibration. Results were quoted as average number molecular weight (M_n) and mean weight average molecular weight (M_w).

2.9. Differential scanning calorimetry (DSC) of nanoparticles

Thermal analysis of CUR–DOX–PBCA nanoparticles were used to provide additional information on the polymer–drug relationship and the nature of formed nanoparticles investigated by a differential scanning calorimeter (DSC 200 F3, NETZSCH, Germany) under nitrogen gas at a flow rate of 20 mL/min. Approximately one milligram of samples were sealed into aluminum pans with DSC sample press and heated from 30 °C to 300 °C at a heating rate of 10 °C/min. A blank aluminum cell was used as a reference. The DSC thermograms were also obtained for α-BCA, blank PBCA nanoparticles, pure curcumin and doxorubicin drugs.

2.10. Cytotoxicity study of various formulations

In vitro cytotoxity assays were performed by MTT assay. The following were assessed for their ability to inhibit cell growth: free curcumin solution (CUR), free doxorubicin solution (DOX), nanoparticles containing only doxorubicin or curcumin (DOX–PBCA-NPs, CUR–PBCA-NPs), combinations of two of these formulations (*i.e.* DOX + CUR, CUR + DOX–PBCA-NPs, DOX + CUR–PBCA-NPs, DOX–PBCA-NPs + CUR–PBCA-NPs), and CUR–DOX–PBCA-NPs. Blank PBCA-NPs suspensions without CUR and DOX equivalent to the drug-loaded PBCA nanoparticles were also tested for comparison. Briefly, MCF-7/ADR cells (100 μL) at a density of 3×10^3 cells/well were seeded into a 96-well plate in the complete growth culture medium. After culturing for 12 h, the medium was exchanged with 200 μL medium containing a series of different concentration of various formulations. After a specified period of time (48 h), the culture medium from each well was removed and the cells were washed twice with phosphate buffered saline (PBS). About 200 μL of the complete growth culture medium and 20 μL MTT solution (5 mg/mL in PBS, pH 7.4) were then added to each well. After 4 h of incubation at 37 °C and 5% CO_2, the media were removed and the formazan crystals were solubilized with 150 μL DMSO for 10 min. The amount of formazan was then determined from the optical density at 570 nm by a microscan spectrum (Electro Thermo, Milford, MA, USA). The results were expressed as percentages relative to the result obtained with the non-toxic control. Experiments were performed in triplicate.

2.11. Determination of multidrug resistant proteins

MCF-7/ADR cells were seeded into 100 mm plates in the presence of DOX + CUR, CUR + DOX–PBCA-NPs, DOX + CUR–PBCA-NPs, DOX–PBCA-NPs + CUR–PBCA-NPs, and CUR–DOX–PBCA-NPs at curcumin 0.2 μg/mL and doxorubicin 0.12 μg/mL for 2 days. Cells were washed with PBS and resuspended in ice-cold EBC buffer (0.5% Nonidet P-40, 50 mmol/L Tris, pH 7.6, 120 mmol/L NaCl, 1 mmol/L EDTA, and 1 mmol/L β-mercaptoethanol) with protease inhibitor mixture and lysed by sonication. The lysates were cleared of insoluble material by centrifugation at 14,000 rpm for 10 min at 4 °C. The supernatant was collected and aliquot into sterile

microcentrifuge tubes, kept at −80 °C until it was used. A protein assay to measure protein content was performed by using the bicihonimic acid protein assay kit.

Samples containing 100 μg of protein were added into 4–14% SDS-PAGE. Aliquots of protein corresponding to 100 μg was mixed with SDS-PAGE sample buffer and heated on hot water bath for 5 min. The samples were resolved on a SDS-PAGE. The proteins were transferred on blotting grade nitrocellulose membrane. The membrane was treated with 5% non-fat dry milk and 0.1% PBS-Tween 20 (milk-PBST) for 2 h at room temperature in order to block the non-specific sites on the membrane. Blots were probed with primary antibodies in rabbit polyclonal anti-MDR1 antibody (1:200), rabbit polyclonal anti-MPR1 antibody (1: 200) and rabbit polyclonal anti-ABCG2 antibody (1:100) for overnight at 4 °C. The membrane was then washed in 1 × PBST three times for 5 min each followed by incubation with secondary antibody horseradish peroxidase conjugated donkey anti-rabbit IgG (1: 5000) for 1 h at room temperature. The membrane was washed in 1 × PBST four times for 10 min each; visualization of hybridization was carried out using chemiluminescence's reagent. The blots were exposed to autoradiography films 12.7 cm × 17.8 cm (Kodak X-OMAT BT) and developed.

2.12. Statistical analysis

Each experiment was conducted in triplicate and values were expressed as the mean SD. Comparison between the difference of means was performed by one-way analysis of variance (ANOVA) with the Tukey test applied post hoc for paired comparisons (SPSS 17.0) where p values of 0.05 or less were considered significant.

3. Results and discussion

3.1. Effect of preparation variables on formulation characteristics

3.1.1. Effect of the time interval of curcumin added on drug-loaded nanoparticles

In this study, the effect of five preparation variables on the mean diameter, zeta potential, loading efficiency and entrapment efficiency of CUR–DOX–PBCA-NPs was investigated. The results are shown in Table 1.

This work was undertaken to investigate the ability for PBCA nanoparticles to incorporate DOX and CUR in one single formulation. In contrast to DOX, when CUR was added immediately prior to the polymerization reaction a marked precipitation was observed. Thus, CUR was added at least 10 min from the beginning of the polymerization process to prevent drug precipitation and polymer aggregation while allowing drug incorporation within the polymeric matrix. Table 1 shows that the encapsulation efficiency of CUR was always close to 95% regardless of the time intervals from the initiation of the polymerization reaction (15, 30, 60 or 120 min) and the particle size decreased and remained unchanged for 60 min. While the encapsulation efficiency of DOX had a little change and arrived at the maximum value 49.98% when added the CUR solution 1 h later the polymerization reaction began.

3.1.2. Effect of the content of chitosan and α-BCA on drug-loaded nanoparticles

The effects of the concentration of chitosan on various parameters of CUR–DOX–PBCA nanoparticles prepared by an emulsion process are shown in Table 1. The zeta potential increased from 32.87 to 40.7 mV, the encapsulation efficiency of CUR increased from 87.38% to 97.3%, and the encapsulation efficiency of DOX increased from 8.35% to 65.22% as the concentration of chitosan in aqueous solution was varied from 0.05% to 0.2% (w/v). The size and loading efficiency of CUR decreases as the concentration of the surfactant increases. While the loading efficiency of DOX arrived at the maximum 0.619% at the chitosan concentration of 0.1%. At low surfactant concentration, the PBCA nanoparticles with porous surfaces would loss drugs from the surface into the suspension medium by diffusion. As the surfactant concentration increased, the porous surfaces of the PBCA nanoparticles gradually became smooth (Mitra and Lin, 2003), and therefore minimized the loss of drug during synthesis. Meanwhile, the particle size decreased as the surfactant concentration increased, resulting in an increase in the total particulate surface area, which promoted the total drug loss from the particles.

The positively charged nanoparticles may have improved stability in the presence of biological cations and may be favorable for some drugs due to their interaction with negatively charged biological membranes and site-specific targeting *in vivo*. Chitosan has been used in the preparation and stabilization of polyester nanocapsules. It has been reported that polymerization of alkyl cyanoacrylates might occur via an anionic mechanism, a zwitterionic mechanism or both of them (Vauthier et al., 2003; Graf et al., 2009). Chitosan-containing amino and hydroxyl groups might act as nucleophilic agents to initiate the butyl cyanoacrylate monomer and is therefore present in the final polymer as end group according to the zwitterionic mechanism, resulting in characteristic change of this PBCA nanoparticle. It was observed that an increase in monomer concentration led to an increased percent drug entrapment of curcumin and doxorubicin, but decreased the drug loading percent. It was also observed that an increase in the amount of monomer led to an increase in particle size, while an increase in the amount of stabilizer resulted in a decrease in particle size of CUR–DOX–PBCA NPs. This effect can be attributed to the mechanism of particle formation mentioned above (Sullivan and Birkinshaw, 2004; Behan et al., 2001).

3.1.3. Content of curcumin and doxorubicin in DOX–CUR–PBCA nanoparticles

Table 1 shows that the content of CUR and DOX in the CUR–DOX–PBCA nanoparticles considerably affect the particle size, the zeta potential, the encapsulation capacity and drug loading in nanoparticles.

In the conventional emulsion method, in order to have high loading efficiency, large amount of feed drug is required. As shown in Table 1, the encapsulation capacity and drug loading of curcumin in CUR–DOX–PBCA nanoparticles were increased from 87.8% to 96.56%, 0.216% to 1.49% respectively, as the curcumin content increased from 0.005% to 0.02%. While the incorporation of curcumin in the polymerization medium, the encapsulation capacity of doxorubicin into the nanoparticles decreased from 53.32% to 42.15%. This observation suggests that during the preparation of CUR–DOX–PBCA-NPs, the incorporation of curcumin in the polymerization medium hindered doxorubicin to take part in the polymerization process.

The encapsulation capacity and drug loading of doxorubicin in CUR–DOX–PBCA-NPs were increased as the doxorubicin content increased, according to the conventional emulsion method. While the incorporation of doxorubicin in the polymerization medium did not significantly affect curcumin encapsulation efficiency into the nanoparticles: CUR (EC%) changed only from 95.14% to 93.97%.

Moreover, the combined formulation of CUR–DOX–PBCA-NPs presented encapsulation contents close to those of each individual drug loaded formulation, which is in good agreement with the previous report (Duan et al., 2010).

3.2. Morphological characterization

Transmission electron micrographs of CUR–DOX–PBCA-NPs are shown in Fig. 1. The nanoparticles are spherical in shape with a

Table 1
Effect of various processing parameters on the particle size, zeta potential, drug encapsulate capacity and drug loading of CUR–DOX–PBCA nanoparticles.

Processing parameters		Characterization					
		DOX (EC%)	DOX (DL%)	CUR (EC%)	CUR (DL%)	Zeta potential (mV)	Particle size (nm)
Time interval of curcumin added	0 min	43 ± 3.21	0.517 ± 0.05	94.65 ± 2.12	1.138 ± 0.04	+37.93 ± 2.43	172 ± 8.56
	15 min	40.12 ± 2.54	0.466 ± 0.02	94.39 ± 2.34	1.049 ± 0.03	+33.4 ± 3.41	160 ± 5.23
	30 min	41.72 ± 2.64	0.29 ± 0.02	93.26 ± 2.67	0.648 ± 0.02	+37.4 ± 4.25	154 ± 6.12
	60 min	49.98 ± 3.32	0.619 ± 0.05	94.52 ± 3.14	1.17 ± 0.04	+32.23 ± 4.56	133 ± 5.34
	120 min	48.12 ± 3.56	0.564 ± 0.02	95.21 ± 3.98	1.013 ± 0.04	+26.13 ± 2.31	130 ± 5.45
Content of α-BCA	0.5%	42.47 ± 2.13	0.694 ± 0.04	94.99 ± 2.98	1.552 ± 0.06	+27.1 ± 2.09	132 ± 4.29
	1.0%	49.98 ± 3.32	0.619 ± 0.05	94.52 ± 3.14	1.17 ± 0.04	+32.23 ± 4.56	133 ± 5.34
	2.0%	53.78 ± 3.24	0.42 ± 0.02	95.44 ± 1.89	0.746 ± 0.02	+32.4 ± 2.16	156 ± 6.34
Content of chitosan	0.05%	8.35 ± 1.12	0.117 ± 0.01	87.38 ± 1.63	1.227 ± 0.02	+32.87 ± 3.18	143 ± 5.49
	0.1%	49.98 ± 3.32	0.619 ± 0.05	94.52 ± 3.14	1.17 ± 0.04	+36.23 ± 4.56	138 ± 5.34
	0.2%	65.22 ± 4.56	0.257 ± 0.02	97.3 ± 2.45	0.384 ± 0.01	+40.7 ± 4.01	133 ± 7.26
Content of curcumin	0.005%	53.32 ± 3.42	0.262 ± 0.02	87.8 ± 2.13	0.216 ± 0.01	+39.47 ± 3.81	138 ± 6.13
	0.01%	49.98 ± 3.32	0.619 ± 0.05	94.52 ± 3.14	1.17 ± 0.04	+32.23 ± 4.56	133 ± 5.34
	0.02%	42.15 ± 3.87	0.402 ± 0.03	96.56 ± 3.01	1.49 ± 0.02	+34.17 ± 2.98	128 ± 7.09
Content of doxorubicin	0.005%	28.18 ± 2.13	0.182 ± 0.01	95.14 ± 3.67	1.226 ± 0.01	+31.07 ± 1.89	120 ± 6.03
	0.01%	49.98 ± 3.32	0.619 ± 0.05	94.52 ± 3.14	1.17 ± 0.04	+32.23 ± 4.56	133 ± 5.34
	0.02%	48.5 ± 3.09	0.709 ± 0.06	93.97 ± 2.26	0.614 ± 0.02	+34.87 ± 2.06	150 ± 7.19

EC%, encapsulation capacity %; DL%, drug loading %.

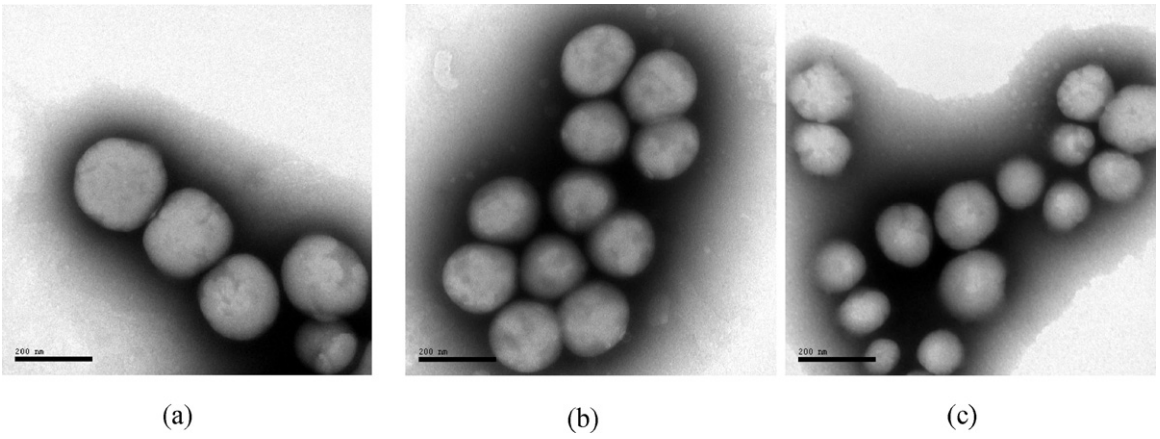

Fig. 1. Transmission electron microscopy (TEM) of CUR–PBCA nanoparticles (a), DOX–PBCA nanoparticles (b), and CUR–DOX–PBCA nanoparticles (c).

smooth surface. The size of CUR–DOX–PBCA-NPs (133 ± 5.34 nm) was smaller than that of CUR–PBCA-NPs (190 ± 5.5 nm) and DOX–PBCA-NPs (174 ± 8.23 nm). This is likely due to the interaction of DOX with the monomer, as it was previously shown that DOX increased the polymerization reaction rate leading to smaller nanoparticle size (Soma et al., 2000). This observation suggested that the incorporation of CUR in the polymerization medium during the preparation of CUR–DOX–PBCA-NPs, hindered DOX to take part in the polymerization process, leading to smaller particle size than that of DOX–PBCA-NPs.

3.3. FT-IR study

FTIR spectroscopy is an appropriate technique to understand chemical adsorption or functionalization of nanoparticles with polymers. As shown from Fig. 2, the CUR–DOX–PBCA-NPs have the similar FTIR spectroscopy as the blank PBCA nanoparticles. The characteristic C≡N stretching at about 2250 cm^{-1} could be readily identified in the spectra of blank PBCA nanoparticles (Fig. 2c, 2250.91 cm^{-1}) and CUR–DOX–PBCA-NPs (Fig. 2d, 2251.47 cm^{-1}). This supported the polymerization mechanism that —CN did not participate any chemical reaction (Behan et al., 2001). The physical mixture of DOX, CUR and blank PBCA nanoparticles has similar spectroscopy to the free doxorubicin and free curcumin, but different from CUR–DOX–PBCA-NPs. The free doxorubicin (Fig. 2b) has an IR absorption band at 1621 cm^{-1}, 1585.10 cm^{-1}, which can be seen in the mixture (Fig. 2e) of 1625.44 cm^{-1} and 1589.92 cm^{-1} due to the stretching vibration of two carbonyl groups of the anthracene ring. Meanwhile, the peak at 3414.71 cm^{-1} which was

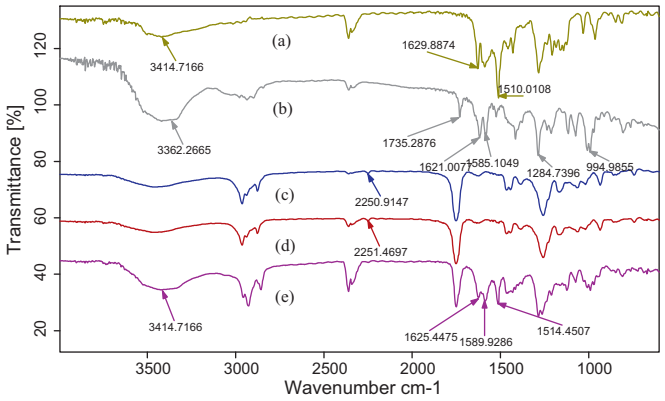

Fig. 2. Fourier-Transform IR (FTIR) spectra of curcumin (a), doxorubicin (b), blank PBCA nanoparticles (c), CUR–DOX–PBCA nanoparticles (d), physical mixture of free doxorubicin, crude curcumin and blank PBCA nanoparticles (e).

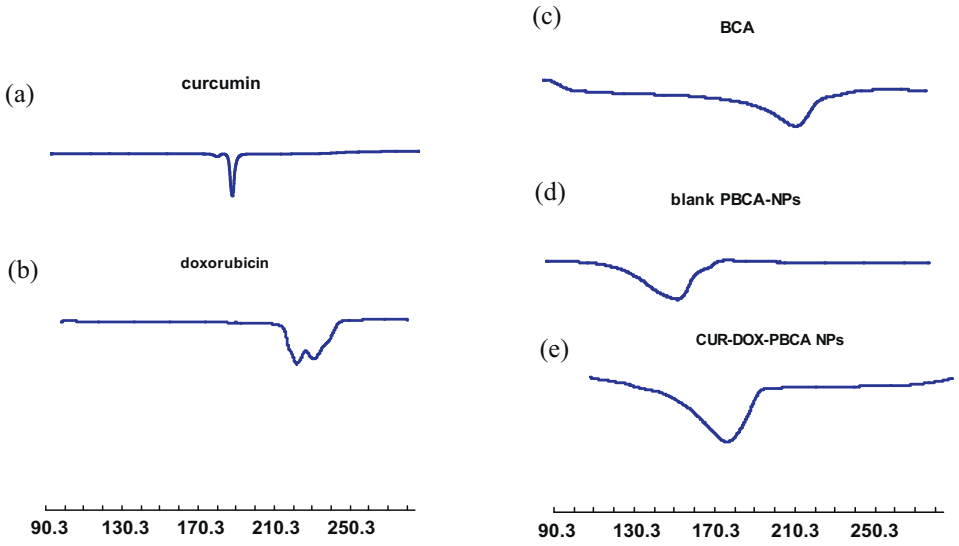

Fig. 3. Differential scanning calorimetry (DSC) thermograms of free curcumin (a), free doxorubicin (b), α-BCA (c), blank PBCA nanoparticles (d), and CUR–DOX–PBCA nanoparticles (e).

found in the spectrum of crude curcumin (Fig. 2a) for phenolic hydroxyl group, and the C=C band of benzene with a stronger absorption peak at 1510.01 cm^{-1} was covered in spectrum of mixture (1514.45 cm^{-1}). However, these peaks disappeared in the spectrum of CUR–DOX–PBCA nanoparticles, which could be a strong evidence for curcumin loaded in nanoparticles. And this result illustrated that doxorubicin is not adhere to the surface of the PBCA nanoparticles, but participate the polymerization of PBCA nanoparticles.

3.4. DSC study

Thermal analysis by DSC can be used to ascertain the physicochemical status of drug in the preparation (Lv et al., 2009). Fig. 3 shows the DSC thermograms of free curcumin, free doxorubicin, α-BCA, blank PBCA nanoparticles and CUR–DOX–PBCA nanoparticles, which can confirm the complete polymerization of monomer and entrapment of curcumin and doxorubicin inside the nanoparticles in molecular dispersion form (Sullivan and Birkinshaw, 2004). From Fig. 3, it is seen that a single sharp endothermic peak was exhibited at about 186.2 °C for CUR with the ΔH value of 504.6 J/g, as the crude curcumin exists as crystals in natural state (Fig. 3a). There are also two endothermic peaks at about 222.26 and 231.66 °C with 945.3 J/g ΔH value for free doxorubicin (Fig. 3b). However, from the graph of CUR–DOX–PBCA nanoparticles (Fig. 3e), a broadened endothermic peak was observed at about 163.6 °C with 227.5 J/g ΔH value. No endothermic peak for curcumin and doxorubicin were obtained, indicating that CUR and DOX loaded in the nanoparticles existed as an amorphous state or a solid solution in the polymeric matrix not a crystalline state. The endothermic peak of BCA monomer was found to be 218.1 °C (Fig. 3c), while that of blank PBCA nanoparticles and CUR–DOX–PBCA nanoparticles was 156.9 °C (Fig. 3d) and 163.6 °C, respectively. The shifting of peak for PBCA nanoparticles compared to the peak of α-BCA monomer revealed that the free monomer was not present in the blank PBCA and CUR–DOX–PBCA nanoparticles suggesting complete polymerization. Moreover, the ΔH value for α-BCA monomer was 2425 J/g. From these ΔH values, it suggests that the prepared blank PBCA nanoparticles and CUR–DOX–PBCA nanoparticles needed less energy for melting compared to curcumin, doxorubicin and BCA monomer, as expected. This provides thermodynamic evidence that curcumin and doxorubicin must be entrapped inside the PBCA nanoparticles. It was reported in the previous studies (Lv et al., 2009; Sullivan and Birkinshaw, 2004), if drug was incorporated into nanoparticles, the value of ΔH of drug loaded nanoparticles was lower than that of pure drug.

Table 2
Molecular weight of various kinds of poly(butyl)cyanoacrylate (PBCA) nanoparticles.

Nanoparticles	Molecular weights		Polydispersity (M_w/M_n)
	M_n (Da)	M_w (Da)	
Blank PBCA-NPs	1612	1988	1.234
CUR–PBCA-NPs	1742	1995	1.145
CUR–DOX–PBCA-NPs	1723	1933	1.122
DOX–PBCA-NPs	1888	2122	1.124

3.5. Gel permeation chromatography

Molecular weight determination was carried out using gel permeation chromatography (Behan et al., 2001; Sullivan and Birkinshaw, 2004). Table 2 shows the mean number average molecular weight and mean weight average molecular weight along with polydispersity index for various kinds of PBCA nanoparticles. Fig. 4 shows the polymer molecular weight distribution curves for the different kinds of PBCA nanoparticles.

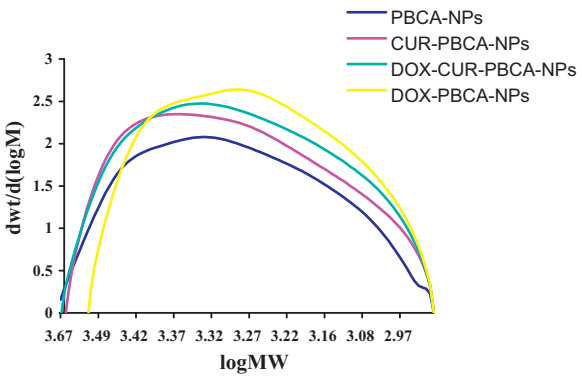

Fig. 4. Molecular weight distribution of blank PBCA nanoparticles, DOX–PBCA nanoparticles, CUR–PBCA nanoparticles and CUR–DOX–PBCA nanoparticles.

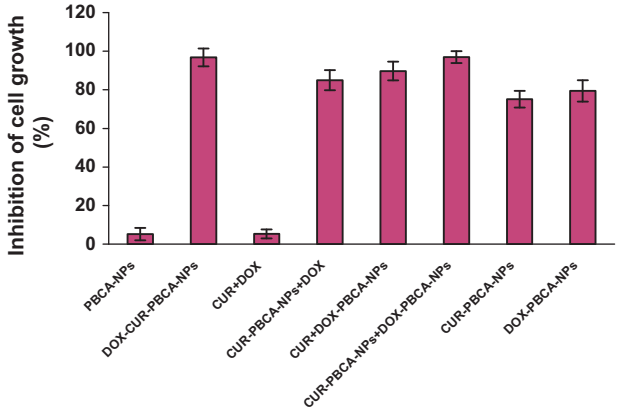

Fig. 5. The inhibition activity of cell growth of different formulations containing doxorubicin and/or curcumin in MCF-7/ADR human breast cancer cells.

CUR–PBCA nanoparticles displayed no significant differences in molecular weight and molecular weight distribution than that of blank PBCA nanoparticles, strongly suggesting that curcumin did not participate in the polymerization of the BCA monomer (Sullivan and Birkinshaw, 2004). In contrast, the presence of DOX into DOX–PBCA nanoparticles led to an increase of blank PBCA molecular weight. It should be noted that DOX–PBCA nanoparticles have a larger molecular weight fraction (M_n = 1888 Da, Mw = 2122 Da) which is illustrated in Fig. 4. The GPC molecular weight profile of DOX–PBCA nanoparticles was already investigated and reported elsewhere (Vansnick et al., 1985). CUR–DOX–PBCA nanoparticles displayed a molecular weight profile similar to that of CUR–PBCA nanoparticles. The profile obtained in our study confirmed the previous results. Thus, as assumed above from the results of particle size data, FTIR and DSC, the GPC results also suggested that curcumin might partly prevent the involvement of doxorubicin in the polymerization process.

3.6. Cytotoxicity studies of various formulations

Fig. 5 presented growth inhibition of P-gp overexpressing MCF-7/ADR cells treated with different formulations containing curcumin 0.2 μg/mL and doxorubicin 0.12 μg/mL for 48 h. The inhibition percents of cell growth of four treatments containing nanoparticle formulation (CUR–DOX–PBCA-NPs, CUR + DOX–PBCA-NPs, DOX + CUR–PBCA-NPs, CUR–PBCA-NPs + DOX–PBCA-NPs) were higher than the free DOX/CUR–PBCA NPs and the free drug combination (CUR + DOX). While blank PBCA nanoparticles at the same concentration caused cell death scarcely, which indicated that the cytotoxicity of drug carrier PBCA-NPs was resulted from curcumin and doxorubicin component rather than the carrier material (PBCA) or surfactant (chitosan). It is clear that curumin co-encapsulated to enhance the ability of DOX–PBCA-NPs to inhibit resistant cell MCF-7/ADR growth. They caused the highest cell death after treatment for 48 h. The results showed that the dual-agent loaded PBCA-NPs system had the similar cytotoxicity (inhibition is 96.94%) to co-administration of two single-agent loaded PBCA-NPs (DOX–PBCA-NPs + CUR–PBCA-NPs, which inhibition is 96.78%), which was slightly higher than that of the free drug nanoparticles (89.43% of DOX–PBCA nanoparticles and 85.15% of CUR–PBCA nanoparticles) and one free drug/another agent loaded PBCA-NPs combination (DOX + CUR–PBCA-NPs, 84.94% or CUR + DOX–PBCA-NPs, 89.72%). Multidrug-resistant can be enhanced by treated combination of encapsulated cytotoxic drugs and reversal agents.

This phenomenon was also possibly relevant to the mechanism of PBCA nanoparticles. It has been previously shown that the degradation of the PACA carrier was shown to play a key role in the mechanism of action (Lenaerts et al., 1984; Muller et al., 1990; Kante et al., 1982). As discussed in the previous paper (Soma et al., 2000), the enhanced activity of the drug-loaded nanoparticles was interpreted as a result of a synergistic effect due to the rapid release of a high amount of curcumin at the surface of the cell membrane, facilitating intracellular diffusion of doxorubicin, leading to drug concentrations at the cell surface higher than those obtained with the same amount of drug diluted in the culture medium, leading in turn to higher intracellular drug concentration. This explains why curcumin in solution failed to enhance the growth inhibition of DOX–PBCA nanoparticles.

The association of curcumin with doxorubicin nanospheres would also ensure that curcumin reaches the same sites as the anticancer drug at the same time and also reduce its toxic side-effects. Co-encapsulating of anticancer drug and reversal agent might cause lower normal tissue drug toxicity and fewer drug-drug interactions. Therefore, we speculate that CUR–DOX–PBCA nanoparticles might be more effective than the other nanoparticle formulations in the treatment of drug resistant cancers *in vivo*.

3.7. CUR–DOX–PBCA nanoparticles affects the multidrug resistant protein expression

Breast cancer cells are usually sensitive to cytotoxic drugs, and combination chemotherapy has been the key therapeutic measure, by which survival rate and quality of life were significantly improved in breast cancer patients. However, cancer cells frequently develop drug resistance after prolonged exposure to cytotoxic drugs. Now, chemoresistance remains a major obstacle to solve in the therapy of many cancer types. One of the major mechanisms of MDR is the enhanced ability of tumor cells to actively efflux drugs, leading to a decrease in cellular drug accumulation below toxic levels. Active drug efflux is mediated by several members of the ATP-binding cassette (ABC) superfamily of membrane transporters, the classical MDR is attributed to the elevated expression of P-gp, MRP1, and ABCG2 (Lage, 2003).

A western blotting analysis of Fig. 6a for the level of P-gp, MRP1 and ABCG2 proteins in MCF-7 and MCF-7/ADR cell lines showed that the drug-resistant MCF-7/ADR cells expressed large amounts of P-gp compared with the drug-sensitive MCF-7 cells, while MRP1 and ABCG2 proteins have a moderate expression. P-gp protein expression was undetectable in MCF-7 cells by the method used in our experiments.

Cancer treatment has led to the investigation of the inhibiting properties of several compounds on these transporters. Although these agents are effective, one of the major problems is their severe toxic side effects. Curcumin has been described as a potent antioxidant, anti-inflammatory agent, and as a significant chemosensitizer in cancer chemotherapy. The compound has been found to be pharmacologically safe and all of these studies suggest that curcumin has enormous potential in the prevention and therapy of cancer (Aggarwal and Harikumar, 2009; Aggarwal et al., 2003; Kunnumakkara et al., 2008).

Fig. 6b shows that after treatment with nanoparticles formulation (CUR–DOX–PBCA-NPs, CUR + DOX–PBCA-NPs, DOX + CUR–PBCA-NPs, CUR–PBCA-NPs + DOX–PBCA-NPs), the expression levels of P-gp in MCF-7/ADR cells were declined, the lowest level being treated with CUR–DOX–PBCA-NPs. The expression of ABCG2 protein has a little declined when MCF-7/ADR cells were cultured with co-encapsulated CUR–DOX–PBCA-NPs. However, no change in MRP1 protein expression level was detected in nanoparticles formulation-treated MCF-7/ADR cells, indicating that the reversal effect of various kinds of PBCA nanoparticles on MDR in MCF-7/ADR cells cannot result from modulating the expression of MRP1.

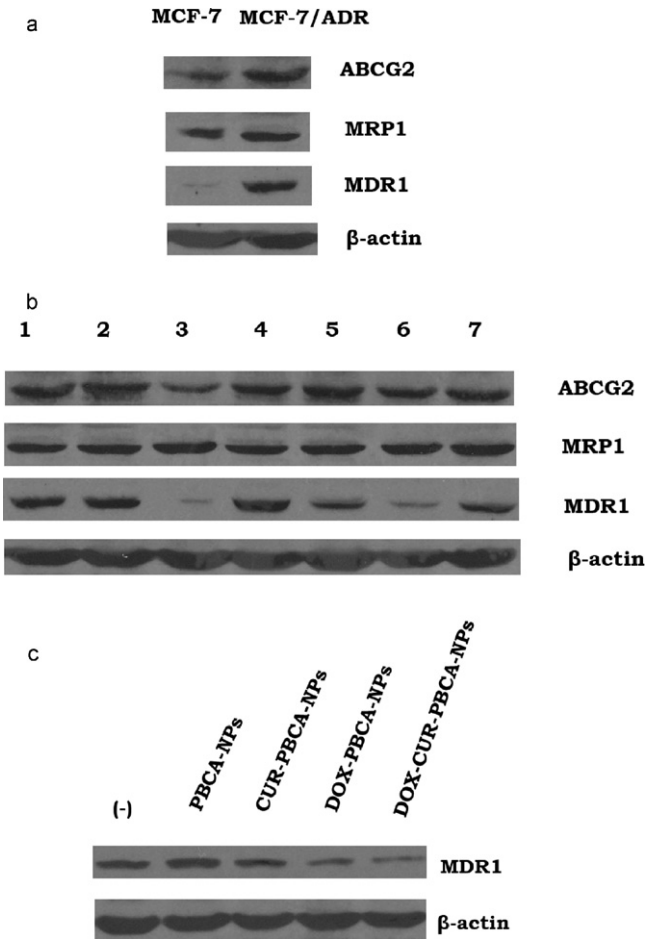

Fig. 6. (a) Expression of MDR1, MRP1 and ABCG2 proteins in MCF-7 cells and MCF-7/ADR cells. (b) Effects of MCF-7/ADR cells on MDR1, MRP1, ABCG2 expression of various kinds of nanoparticle formulations. (1) Control; (2) PBCA-NPs; (3) CUR–DOX–PBCA-NPs; (4) CUR + DOX; (5) CUR–PBCA-NPs + DOX; (6) CUR–PBCA-NPs + DOX–PBCA-NPs; (7) DOX–PBCA-NPs + CUR. (c) Analysis of MDR1 protein in MCF-7/ADR cells.

The overexpression of P-gp in tumor cell membrane is considered to be the major mechanism of MDR. P-gp is able to pump various anticancer drugs, such as doxorubicin, out of cells, thus resulting in a low intracellular drug concentration that is insufficient to kill tumor cells. While about the reversing MDR mechanism of DOX–PACA nanoparticles, illustrated in the reference (De Verdiere et al., 1997), that doxorubicin is able to form ion pairs with the degradation product of PACA, which leads to a modified permeability of the anthracycline across membranes. This is probably the reason why, to date, only PACA nanoparticles fulfill these requirements and overcome the resistance caused by the P-gp (De Verdiere et al., 1997). To use compounds with low or no toxicity to bind P-gp and block its transport function is the most common method of reversing MDR. Curcumin was examined here to determine possible interactions with P-gp expression and function. The inhibition of P-gp by curcumin might provide a novel approach for reversing MDR in tumor cells.

In such a co-culture, the doxorubicin-loaded nanoparticles by themselves can only partially overcome the MDR. The enhanced activity of the drug-loaded nanoparticles was also illustrated by the result of Fig. 6c. The association of curcumin with doxorubicin nanospheres would also ensure that curcumin reaches the same sites as the anticancer drug at the same time while reducing its toxic side effects.

4. Conclusions

In this paper, we report for the first time that two drugs with different properties (CUR and DOX·HCl, hydrophobic and hydrophilic molecules, respectively) can be simultaneously entrapped into chitosan–PBCA nanoparticles with a relatively high-entrapment efficiency and small size. The influences of various processing variables on particle size, zeta potential, drug loading and encapsulation capacity were systematically assessed.

Using chitosan–PBCA nanoparticles as a novel drug delivery platform, various strategies for administering DOX/CUR combinations were systematically compared. It was found that the dual-agent loaded CUR–DOX–PBCA-NPs system resulted in similar cytotoxicity to co-administration of two single-agent loaded PBCA-NPs (CUR–PBCA-NPs + DOX–PBCA-NPs), and slightly higher cytotoxicity than that of the free DOX/CUR–PBCA-NPs and one free drug/another agent loaded PBCA-NPs combination (CUR + DOX–PBCA-NPs or CUR–PBCA-NPs + DOX). The data obtained in this study have shown that the simultaneous administration of an anticancer compound (DOX) and a chemosensitizer (CUR) could improve the efficacy of doxorubicin nanoparticles in overcoming MDR and achieve the highest reversal efficacy. Co-encapsulation of anticancer drug and chemosensitizer might cause lower normal tissue drug toxicity and fewer drug–drug interactions. We are currently investigating tissue distribution properties and *in vivo* reversal efficacy of dual agent CUR–DOX–PBCA-NPs and co-administration of two single-agent loaded PBCA-NPs.

Acknowledgment

This study was supported by a Lotus Scholars Program (200734) in Hunan Province, PR China.

References

Aggarwal, B.B., Harikumar, K.B., 2009. Potential therapeutic effects of curcumin, the anti-inflammatory agent, against neurodegenerative, cardiovascular, pulmonary, metabolic, autoimmune and neoplastic diseases. Int. J. Biochem. Cell Biol. 1, 40–59.

Aggarwal, B.B., Kumar, A., Bharti, A.C., 2003. Anticancer potential of curcumin: preclinical and clinical studies. Anticancer Res. 23, 363–398.

Ambruosi, A., Gelperina, S., Khalansky, A., Tanski, S., Theisen, A., Kreuter, J., 2006. Influence of surfactants, polymer and doxorubicin loading on the anti-tumour effect of poly(butyl cyanoacrylate) nanoparticles in a rat glioma model. J. Microencapsul. 23, 582–592.

Anand, P., Kunnumakkara, A.B., Newman, R.A., Aggarwal, B.B., 2007. Bioavailability of curcumin: problems and promises. Mol. Pharm. 4, 807–818.

Andjelkovic, T., Pesic, M., Bankovic, J., Tanic, N., Markovic, I.D., Ruzdijic, S., 2008. Synergistic effects of the purine analog sulfinosine and curcumin on the multidrug resistance human non-small cell lung carcinoma cell line (NCI-H460/R). Cancer Biol. Ther. 7, 1024–1032.

Antonio, A., Manuela, I., Carmine, D.I., Franco, C., Ettore, P., 2008. Reversal of P-glycoprotein-mediated multidrug resistance in human sarcoma MES-SA/Dx-5 cells by nonsteroidal anti-inflammatory drugs. Oncol. Rep. 20, 731–735.

Behan, N., Birkinshaw, C., Clarke, N., 2001. Poly *n*-butyl cyanoacrylate nanoparticles: a mechanistic study of polymerisation and particle formation. Biomaterials 22, 1335–1344.

Chen, B.A., Sun, Q., Wang, X.M., Gao, F., Dai, Y.Y., Yin, Y., Ding, J.H., Gao, C., Cheng, J., Li, J.Y., Sun, X.C., Chen, X.C., Xu, W.L., Shen, H.L., Liu, D.L., 2008. Reversal in multidrug resistance by magnetic nanoparticle of Fe_3O_4 loaded with adriamycin and tetrandrine in K562/A02 leukemic cells. Int. J. Nanomed. 3, 277–286.

Cheng, A.L., Hsu, C.H., Lin, J.K., Hsu, M.M., Ho, Y.F., Shen, T.S., Ko, J.Y., Lin, J.T., Lin, B.R., Ming-Shiang, W., Yu, H.S., Jee, S.H., Chen, G.S., Chen, T.M., Chen, C.A., Lai, M.K., Pu, Y.S., Pan, M.H., Wang, Y.J., Tsai, C.C., Hsieh, C.Y., 2001. Phase I clinical trial of curcumin, a chemopreventive agent, in patients with high-risk or pre-malignant lesions. Anticancer Res. 21, 2895–2900.

De Verdiere, A.C., Dubernet, C., Nemati, F., Soma, E., Appel, M., FertA., J., Bernard, S., Puisieux, F., Couvreur, P., 1997. Revertion of multidrug resistance with polyalkylcyanoacrylate nanoparticles: towards a mechanism of action. Br. J. Cancer 76, 198–205.

Dong, X.W., Mumper, R.J., 2010. Nanomedicinal strategies to treat multidrug-resistant tumors: current progress. Nanomedicine 5, 597–615.

Dong, X.W., Mattingly, C.A., Tseng, M.T., Cho, M.J., Liu, Y., Adams, V.R., Mumper, R.J., 2009. Doxorubicin and paclitaxel-loaded lipid-based nanoparticles overcome

multidrug resistance by inhibiting P-glycoprotein and depleting ATP. Cancer Res. 69, 3918–3926.
Duan, J.H., Zhang, Y.D., Han, S.W., Chen, Y.X., Li, B., Liao, M.M., Chen, W., Deng, X.M., Zhao, J.F., Huang, B.Y., 2010. Synthesis and in vitro/in vivo anti-cancer evaluation of curcumin-loaded chitosan/poly(butyl cyanoacrylate) nanoparticles. Int. J. Pharm. 400, 211–220.
Ebert, B., Seidel, A., Lampen, A., 2007. Phytochemicals induce breast cancer resistance protein in Caco-2 cells and enhance the transport of benzo[a]pyrene-3-sulfate. Toxicol. Sci. 96, 227–236.
Ganta, S., Amiji, M., 2009. Coadministration of paclitaxel and curcumin in nanoemulsion formulations to overcome multidrug resistance in tumor cells. Mol. Pharm. 6, 928–939.
Graf, A., McDowell, A., Rades, T., 2009. Poly(alkycyanoacrylate) nanoparticles for enhanced delivery of therapeutics—is there real potential? Expert Opin. Drug Deliv. 6, 371–387.
Gu, F.X., Karnik, R., Wang, A.Z., Alexis, F., Levy-Nissenbaum, E., Hong, S., Langer, R.S., Farokhzad, O.C., 2007. Targeted nanoparticles for cancer therapy. Nano Today 2, 14–21.
Hou, X.L., Takahashi, K., Tanaka, K., Tou gou, K., Qiu, F., Komatsu, K., Takahashi, K., Azuma, J., 2008. Curcuma drugs and curcumin regulate the expression and function of P-gp in Caco-2 cells in completely opposite ways. Int. J. Pharm. 358, 224–229.
Kang, K.W., Chun, M.K., Kim, O., Subedi, R.K., Ahn, S.G., Yoon, J.H., Choi, H.K., 2010. Doxorubicin-loaded solid lipid nanoparticles to overcome multidrug resistance in cancer therapy. Nanomed. Nanotechnol. 6, 210–213.
Kante, B., Couvreur, P., Dubois-Krack, G., De Meester, C., Guiot, P., Roland, M., Mercier, M., Speiser, P., 1982. Degradation of polyalkylcyanoacrylate nanoparticles I: free nanoparticles. J. Pharm. Sci. 71, 786–790.
Kunnumakkara, A.B., Anand, P., Aggarwal, B.B., 2008. Curcumin inhibits proliferation, invasion, angiogenesis and metastasis of different cancers through interaction with multiple cell signaling proteins. Cancer Lett. 269, 199–225.
Lage, H., 2003. ABC-transporters: Implications on drug resistance from microorganisms to human cancers. Int. J. Antimicrob. Agents 22, 188–199.
Lenaerts, V., Couvreur, P., Christiaens-Leyh, D., Joiris, E., Roland, M., Rollman, B., Speiser, P., 1984. Degradation of poly(isobutylcyanoacrylate) nanoparticles. Biomaterials 5, 65–68.
Lv, Q.Z., Yu, A.H., Xi, Y.W., Li, H.L., Song, Z.M., Cui, J., Cao, F.L., Zhai, G.X., 2009. Development and evaluation of penciclovir-loaded solid lipid nanoparticles for topical delivery. Int. J. Pharm. 372, 191–198.
Mitra, A., Lin, S.S., 2003. Effect of surfactant on fabrication and characterization of paclitaxel-loaded polybutylcyanoacrylate nanoparticulate delivery systems. J. Pharm. Pharmacol. 55, 895–902.
Muller, R.H., Lherm, C., Herbert, J., Couvreur, P., 1990. In vitro model for the degradation of alkylcyanoacrylate nanoparticles. Biomaterials 11, 590–595.
Notarbartolo, M., Poma, P., Perri, D., Dusonchet, L., Cervello, M., D'Alessandro, N., 2005. Antitumor effects of curcumin, alone or in combination with cisplatin or doxorubicin, on human hepatic cancer cells. Analysis of their possible relationship to changes in NF-κB activation levels and in IAP gene expression. Cancer Lett. 1, 53–65.
Reddy, L.H., Sharma, R.K., Murthy, R.S.R., 2004. Enhanced tumour uptake of doxorubicin loaded poly(butyl cyanoacrylate) nanoparticles in mice bearing Dalton's Lymphoma tumour. J. Drug Target. 12, 443–451.
Soma, C.E., Dubernet, C., Bentolila, D., Benita, S., Couvreur, P., 2000. Reversion of multidrug resistance by co-encapsulation of doxorubicin and cyclosporin A in polyalkylcyanoacrylate nanoparticles. Biomaterials 21, 1–7.
Song, X.R., Cai, Z., Zheng, Y., He, G., Cui, F.Y., Gong, D.Q., Hou, S.X., Xiong, S.J., Lei, X.J., Wei, Y.Q., 2009. Reversion of multidrug resistance by co-encapsulation of vincristine and verapamil in PLGA nanoparticles. Eur J. Pharm. Sci. 37, 300–305.
Sullivan, C.O., Birkinshaw, C., 2004. In vitro degradation of insulin-loaded poly(n-butylcyanoacrylate) nanoparticles. Biomaterials 25, 4375–4382.
Tang, H.D., Murphy, C.J., Shen, Y.Q., Sui, M.H., Kirk, E.A.V., Feng, X.W., Murdoch, W.J., 2010. Amphiphilic curcumin conjugate-forming nanoparticles as anticancer prodrug and drug carriers: *in vitro* and *in vivo* effects. Nanomedicine 5, 855–865.
Vansnick, L., Couvreur, P., Christiaens-Leyh, D., Roland, M., 1985. Molecular weights of free and drug-loaded nanoparticles. Pharm. Res. 1, 36–41.
Vauthier, C., Dubernet, C., Fattal, E., Pinto-Alphandary, H., Couvreur, P., 2003. Poly(alkylcyanoacrylates) as biodegradable materials for biomedical applications. Adv. Drug Deliv. Rev. 55, 519–548.
Wohlgemuth, M., Machtle, W., Mayer, C., 2000. Improved preparation and physical studies of polybutylcyanoacrylate nanocapsules. J. Microencapsul. 17, 437–448.
Wu, J., Lu, Y.H., Lee, A., Pan, X.G., Yang, X.J., Zhao, X.B., Lee, R.J., 2007. Reversal of multidrug resistance by transferring-conjugated liposomes co-encapsulating doxorubicin and verapamil. J. Pharm. Pharm. Sci. 10, 350–357.